Vibration and buckling of composite beams using refined shear deformation theory

Thuc P. Vo[a,b,*], Huu-Tai Thai[c]

[a] *School of Mechanical, Aeronautical and Electrical Engineering, Glyndŵr University, Mold Road, Wrexham LL11 2AW, UK.*
[b] *Advanced Composite Training and Development Centre, Unit 5, Hawarden Industrial Park Deeside, Flintshire CH5 3US, UK.*
[c] *Department of Civil and Environmental Engineering, Hanyang University, 17 Haengdang-dong, Seongdong-gu, Seoul 133-791, Republic of Korea.*

Abstract

Vibration and buckling analysis of composite beams with arbitrary lay-ups using refined shear deformation theory is presented. The theory accounts for the parabolical variation of shear strains through the depth of beam. Three governing equations of motion are derived from the Hamilton's principle. The resulting coupling is referred to as triply coupled vibration and buckling. A two-noded C^1 beam element with five degree-of-freedom per node which accounts for shear deformation effects and all coupling coming from the material anisotropy is developed to solve the problem. Numerical results are obtained for composite beams to investigate effects of fiber orientation and modulus ratio on the natural frequencies, critical buckling loads and corresponding mode shapes.

Keywords: Composite beams; refined shear deformation theory; triply coupled vibration and buckling.

1. Introduction

Structural components made with composite materials are increasingly being used in various engineering applications due to their attractive properties in strength, stiffness, and lightness. Understanding their dynamic and buckling behaviour is of increasing importance. The classical beam theory (CBT) known as Euler-Bernoulli beam theory is the simplest one and is applicable to slender beams only. For moderately deep beams, it overestimates buckling loads and natural frequencies due to ignoring the transverse shear effects. The first-order beam theory (FOBT) known as Timoshenko beam theory is proposed to overcome the limitations of the CBT by accounting for the transverse shear effects. Since the FOBT violates the zero shear stress conditions on the top and bottom surfaces of

*Corresponding author, tel.: +44 1978 293979
Email address: t.vo@glyndwr.ac.uk (Thuc P. Vo)

the beam, a shear correction factor is required to account for the discrepancy between the actual stress state and the assumed constant stress state. To remove the discrepancies in the CBT and FOBT, the higher-order beam theory (HOBT) is developed to avoid the use of shear correction factor and have a better prediction of response of laminated beams. The HOBTs can be developed based on the assumption of higher-order variations of in-plane displacement or both in-plane and transverse displacements through the depth of the beam. Many numerical techniques have been used to solve the dynamic and/or buckling analysis of composite beams using HOBTs. Some researchers studied the free vibration characteristics of composite beams by using finite element ([1]-[7]). Khdeir and Reddy ([8], [9]) developed analytical solutions for free vibration and buckling of cross-ply composite beams with arbitrary boundary conditions in conjunction with the state space approach. Analytical solutions were also derived by Kant et al. ([10], [11]) and Zhen and Wanji [12] to study vibration and buckling of composite beams. By using the method of power series expansion of displacement components, Matsunaga [13] analysed the natural frequencies and buckling stresses of composite beams. Aydogdu ([14]-[16]) carried out the vibration and buckling analysis of cross-ply and angle-ply with different sets of boundary conditions by using Ritz method. Jun et al. ([17],[18]) introduced the dynamic stiffness matrix method to solve the free vibration and buckling problems of axially loaded composite beams with arbitrary lay-ups.

In this paper, which is extended from previous research [19], vibration and buckling analysis of composite beams using refined shear deformation theory is presented. The displacement field is reduced from the so-called Refined Plate Theory developed by Shimpi ([20], [21]) and based on the following assumptions: (1) the axial and transverse displacements consist of bending and shear components in which the bending components do not contribute toward shear forces and, likewise, the shear components do not contribute toward bending moments; (2) the bending component of axial displacement is similar to that given by the CBT; and (3) the shear component of axial displacement gives rise to the higher-order variation of shear strain and hence to shear stress through the depth of the beam in such a way that shear stress vanishes on the top and bottom surfaces. The most interesting feature of this theory is that it satisfies the zero traction boundary conditions on the top and bottom surfaces of the beam without using shear correction factors. The three governing equations of motion are derived from the Hamilton's principle. The resulting coupling is referred to as triply coupled vibration and buckling. A two-noded C^1 beam element with five degree-of-freedom (DOF) per node which accounts for shear deformation effects and all coupling coming from the material anisotropy is developed to solve the problem. Numerical results are obtained for composite beams to investigate effects of fiber orientation and modulus ratio on the natural frequencies, critical buckling loads and

corresponding mode shapes.

2. Kinematics

A laminated composite beam made of many plies of orthotropic materials in different orientations with respect to the x-axis, as shown in Fig. 1, is considered. Based on the assumptions made in the preceding section, the displacement field of the present theory can be obtained as:

$$U(x,z,t) = u(x,t) - z\frac{\partial w_b(x,t)}{\partial x} + z\Big[\frac{1}{4} - \frac{5}{3}\big(\frac{z}{h}\big)^2\Big]\frac{\partial w_s(x,t)}{\partial x} \tag{1a}$$

$$W(x,z,t) = w_b(x,t) + w_s(x,t) \tag{1b}$$

where u is the axial displacement along the mid-plane of the beam, w_b and w_s are the bending and shear components of transverse displacement along the mid-plane of the beam, respectively. The non-zero strains are given by:

$$\epsilon_x = \frac{\partial U}{\partial x} = \epsilon_x^\circ + z\kappa_x^b + f\kappa_x^s \tag{2a}$$

$$\gamma_{xz} = \frac{\partial W}{\partial x} + \frac{\partial U}{\partial z} = (1-f')\gamma_{xz}^\circ = g\gamma_{xz}^\circ \tag{2b}$$

where

$$f = z\Big[-\frac{1}{4} + \frac{5}{3}\big(\frac{z}{h}\big)^2\Big] \tag{3a}$$

$$g = 1 - f' = \frac{5}{4}\Big[1 - 4\big(\frac{z}{h}\big)^2\Big] \tag{3b}$$

and $\epsilon_x^\circ, \gamma_{xz}^\circ, \kappa_x^b, \kappa_x^s$ and κ_{xy} are the axial strain, shear strains and curvatures in the beam, respectively defined as:

$$\epsilon_x^\circ = u' \tag{4a}$$

$$\gamma_{xz}^\circ = w_s' \tag{4b}$$

$$\kappa_x^b = -w_b'' \tag{4c}$$

$$\kappa_x^s = -w_s'' \tag{4d}$$

where differentiation with respect to the x-axis is denoted by primes ($'$).

3. Variational Formulation

In order to derive the equations of motion, Hamilton's principle is used:

$$\delta\int_{t_1}^{t_2}(\mathcal{K} - \mathcal{U} - \mathcal{V})dt = 0 \tag{5}$$

where $\mathcal{U}$ is the strain energy, $\mathcal{V}$ is the potential energy, and $\mathcal{K}$ is the kinetic energy.

The variation of the strain energy can be stated as:

$$\delta\mathcal{U} = \int_v (\sigma_x \delta\epsilon_x + \sigma_{xz}\delta\gamma_{xz})dv = \int_0^l (N_x\delta\epsilon_z^\circ + M_x^b\delta\kappa_x^b + M_x^s\delta\kappa_x^s + Q_{xz}\delta\gamma_{xz}^\circ)dx \tag{6}$$

where N_x, M_x^b, M_x^s and Q_{xz} are the axial force, bending moments and shear force, respectively, defined by integrating over the cross-sectional area A as:

$$N_x = \int_A \sigma_x dA \tag{7a}$$

$$M_x^b = \int_A \sigma_x z dA \tag{7b}$$

$$M_x^s = \int_A \sigma_x f dA \tag{7c}$$

$$Q_{xz} = \int_A \sigma_{xz} g dA \tag{7d}$$

The variation of the potential energy of the axial force P_0, which is applied through the centroid, can be expressed as:

$$\delta\mathcal{V} = -\int_0^l P_0\Big[\delta w_b'(w_b' + w_s') + \delta w_s'(w_b' + w_s')\Big]dx \tag{8}$$

The variation of the kinetic energy is obtained as:

$$\begin{aligned}\delta\mathcal{K} &= \int_v \rho_k(\dot{U}\delta\dot{U} + \dot{W}\delta\dot{W})dv \\ &= \int_0^l \Big[\delta\dot{u}(m_0\dot{u} - m_1\dot{w_b}' - m_f\dot{w_s}') + \delta\dot{w_b}m_0(\dot{w_b} + \dot{w_s}) + \delta\dot{w_b}'(-m_1\dot{u} + m_2\dot{w_b}' + m_{fz}\dot{w_s}') \\ &+ \delta\dot{w_s}m_0(\dot{w_b} + \dot{w_s}) + \delta\dot{w_s}'(-m_f\dot{u} + m_{fz}\dot{w_b}' + m_{f^2}\dot{w_s}')\Big]dx\end{aligned} \tag{9}$$

where the differentiation with respect to the time t is denoted by dot-superscript convention and ρ_k is the density of a k^{th} layer and $m_0, m_1, m_2, m_f, m_{fz}$ and m_{f^2} are the inertia coefficients, defined by:

$$m_f = -\frac{m_1}{4} + \frac{5}{3h^2}m_3 \tag{10a}$$

$$m_{fz} = -\frac{m_2}{4} + \frac{5}{3h^2}m_4 \tag{10b}$$

$$m_{f^2} = \frac{m_2}{16} - \frac{5}{6h^2}m_4 + \frac{25}{9h^4}m_6 \tag{10c}$$

where:

$$(m_0, m_1, m_2, m_3, m_4, m_6) = \int_A \rho_k(1, z, z^2, z^3, z^4, z^6)dA \tag{11}$$

By substituting Eqs. (6), (8) and (9) into Eq. (5), the following weak statement is obtained:

$$\begin{aligned} 0 &= \int_{t_1}^{t_2}\int_0^l \Big[\delta\dot{u}(m_0\dot{u} - m_1\dot{w_b}' - m_f\dot{w_s}') + \delta\dot{w_b}m_0(\dot{w_b}+\dot{w_s}) + \delta\dot{w_b}'(-m_1\dot{u} + m_2\dot{w_b}' + m_{fz}\dot{w_s}') \\ &+ \delta\dot{w_s}m_0(\dot{w_b}+\dot{w_s}) + \delta\dot{w_s}'(-m_f\dot{u} + m_{fz}\dot{w_b}' + m_{f^2}\dot{w_s}') \\ &+ P_0\big[\delta w_b'(w_b'+w_s') + \delta w_s'(w_b'+w_s')\big] - N_x\delta u' + M_x^b\delta w_b'' + M_x^s\delta w_s'' - Q_{xz}\delta w_s'\Big]dxdt \end{aligned} \tag{12}$$

4. Constitutive Equations

The stress-strain relations for the k^{th} lamina are given by:

$$\sigma_x = \bar{Q}_{11}\epsilon_x \tag{13a}$$

$$\sigma_{xz} = \bar{Q}_{55}\gamma_{xz} \tag{13b}$$

where $\bar{Q}_{11}$ and $\bar{Q}_{55}$ are the elastic stiffnesses transformed to the x direction. More detailed explanation can be found in Ref. [22].

The constitutive equations for bar forces and bar strains are obtained by using Eqs. (2), (7) and (13):

$$\begin{Bmatrix} N_x \\ M_x^b \\ M_x^s \\ Q_{xz} \end{Bmatrix} = \begin{bmatrix} R_{11} & R_{12} & R_{13} & 0 \\ & R_{22} & R_{23} & 0 \\ & & R_{33} & 0 \\ \text{sym.} & & & R_{44} \end{bmatrix} \begin{Bmatrix} \epsilon_x^\circ \\ \kappa_x^b \\ \kappa_x^s \\ \gamma_{xz}^\circ \end{Bmatrix} \tag{14}$$

where R_{ij} are the laminate stiffnesses of general composite beams and given by:

$$R_{11} = \int_y A_{11}dy \tag{15a}$$

$$R_{12} = \int_y B_{11}dy \tag{15b}$$

$$R_{13} = \int_y (-\frac{B_{11}}{4} + \frac{5}{3h^2}E_{11})dy \tag{15c}$$

$$R_{22} = \int_y D_{11}dy \tag{15d}$$

$$R_{23} = \int_y (-\frac{D_{11}}{4} + \frac{5}{3h^2}F_{11})dy \tag{15e}$$

$$R_{33} = \int_y (\frac{D_{11}}{16} - \frac{5}{6h^2}F_{11} + \frac{25}{9h^4}H_{11})dy \tag{15f}$$

$$R_{44} = \int_y (\frac{25}{16}A_{55} - \frac{25}{2h^2}D_{55} + \frac{25}{h^4}F_{55})dy \tag{15g}$$

where A_{ij}, B_{ij} and D_{ij} matrices are the extensional, coupling and bending stiffness and E_{ij}, F_{ij}, H_{ij} matrices are the higher-order stiffnesses, respectively, defined by:

$$(A_{ij}, B_{ij}, D_{ij}, E_{ij}, F_{ij}, H_{ij}) = \int_z \bar{Q}_{ij}(1, z, z^2, z^3, z^4, z^6)dz \tag{16}$$

5. Governing equations of motion

The equilibrium equations of the present study can be obtained by integrating the derivatives of the varied quantities by parts and collecting the coefficients of $\delta u, \delta w_b$ and δw_s:

$$N_x' = m_0\ddot{u} - m_1\ddot{w_b}' - m_f\ddot{w_s}' \tag{17a}$$

$$M_x^{b\prime\prime} - P_0(w_b'' + w_s'') = m_0(\ddot{w_b} + \ddot{w_s}) + m_1\ddot{u}' - m_2\ddot{w_b}'' - m_{fz}\ddot{w_s}'' \tag{17b}$$

$$M_x^{s\prime\prime} + Q_{xz}' - P_0(w_b'' + w_s'') = m_0(\ddot{w_b} + \ddot{w_s}) + m_f\ddot{u}' - m_{fz}\ddot{w_b}'' - m_{f^2}\ddot{w_s}'' \tag{17c}$$

The natural boundary conditions are of the form:

$$\delta u : N_x \tag{18a}$$

$$\delta w_b : M_x^{b'} - P_0(wb' + ws') - m_1\ddot{u} + m_2\ddot{w_b}' + m_{fz}\ddot{w_s}' \tag{18b}$$

$$\delta w_b' : M_x^b \tag{18c}$$

$$\delta w_s : M_x^{s'} + Q_{xz} - P_0(wb' + ws') - m_f\ddot{u} + m_{fz}\ddot{w_b}' + m_{f^2}\ddot{w_s}' \tag{18d}$$

$$\delta w_s' : M_x^s \tag{18e}$$

By substituting Eqs. (4) and (14) into Eq. (17), the explicit form of the governing equations of motion can be expressed with respect to the laminate stiffnesses R_{ij}:

$$R_{11}u'' - R_{12}w_b''' - R_{13}w_s''' = m_0\ddot{u} - m_1\ddot{w_b}' - m_f\ddot{w_s}' \tag{19a}$$

$$R_{12}u''' - R_{22}w_b^{iv} - R_{23}w_s^{iv} - P_0(w_b'' + w_s'') = m_0(\ddot{w_b} + \ddot{w_s}) + m_1\ddot{u}' - m_2\ddot{w_b}'' - m_{fz}\ddot{w_s}'' \tag{19b}$$

$$R_{13}u''' - R_{23}w_b^{iv} - R_{33}w_s^{iv} + R_{44}w_s'' - P_0(w_b'' + w_s'') = m_0(\ddot{w_b} + \ddot{w_s}) + m_f\ddot{u}' - m_{fz}\ddot{w_b}'' - m_{f^2}\ddot{w_s}'' \tag{19c}$$

Eq. (19) is the most general form for vibration and buckling of composite beams of composite beams, and the dependent variables, u, w_b and w_s are fully coupled. The resulting coupling is referred to as triply axial-flexural coupled vibration and buckling. It can be seen that the explicit solutions for vibration and buckling of composite beams become complicated due to this triply coupling effect.

6. Finite Element Formulation

The present theory for composite beams described in the previous section is implemented via a displacement based finite element method. The variational statement in Eq. (12) requires that the bending and shear components of transverse displacement w_b and w_s be twice differentiable and C^1-continuous, whereas the axial displacement u must be only once differentiable and C^0-continuous. The generalized displacements are expressed over each element as a combination of the linear interpolation function Ψ_j for u and Hermite-cubic interpolation function $\widehat{\psi_j}$ for w_b and w_s associated with node j and the nodal values:

$$u = \sum_{j=1}^{2} u_j \Psi_j \tag{20a}$$

$$w_b = \sum_{j=1}^{4} w_{bj} \widehat{\psi_j} \tag{20b}$$

$$w_s = \sum_{j=1}^{4} w_{sj} \widehat{\psi_j} \tag{20c}$$

Substituting these expressions in Eq. (20) into the corresponding weak statement in Eq. (12), the finite element model of a typical element can be expressed as the standard eigenvalue problem:

$$([K] - P_0[G] - \omega^2[M])\{\Delta\} = \{0\} \tag{21}$$

where $[K], [G]$ and $[M]$ are the element stiffness matrix, the element geometric stiffness matrix and the element mass matrix, respectively. The explicit forms of $[K]$ can be found in Ref. [19] and of $[G]$ and $[M]$ are given by:

$$G_{ij}^{22} = \int_0^l \psi_i' \psi_j' dz \tag{22a}$$

$$G_{ij}^{23} = \int_0^l \psi_i' \psi_j' dz \tag{22b}$$

$$G_{ij}^{33} = \int_0^l \psi_i' \psi_j' dz \tag{22c}$$

$$M_{ij}^{11} = \int_0^l m_0 \Psi_i \Psi_j dz \tag{22d}$$

$$M_{ij}^{12} = -\int_0^l m_1 \Psi_i \psi_j' dz \tag{22e}$$

$$M_{ij}^{13} = -\int_0^l m_f \Psi_i \psi_j' dz \tag{22f}$$

$$M_{ij}^{22} = \int_0^l m_0 \psi_i \psi_j + m_2 \psi_i' \psi_j' dz \tag{22g}$$

$$M_{ij}^{23} = \int_0^l m_0\psi_i\psi_j + m_{fz}\psi_i'\psi_j' dz \tag{22h}$$

$$M_{ij}^{33} = \int_0^l m_0\psi_i\psi_j + m_{f^2}\psi_i'\psi_j' dz \tag{22i}$$

All other components are zero. In Eq.(21), $\{\Delta\}$ is the eigenvector of nodal displacements corresponding to an eigenvalue:

$$\{\Delta\} = \{u\ w_b\ w_s\}^{\mathrm{T}} \tag{23}$$

7. Numerical Examples

In this section, a number of numerical examples are presented and analysed for verification the accuracy of the present theory and investigation the natural frequencies, critical buckling loads and corresponding mode shapes of composite beams with arbitrary lay-ups. The boundary conditions of beam are presented by C for clamped edge: $u = w_b = w_b' = w_s = w_s' = 0$, S for simply-supported edge: $u = w_b = w_s = 0$ and F for free edge. All laminate are of equal thickness and made of the same orthotropic material, whose properties are as follows:

Material I [3]:

$$E_1 = 241.5\text{GPa}, E_2 = 18.98\text{GPa}, G_{12} = G_{13} = 5.18\text{GPa}, G_{23} = 3.45\text{GPa}, \nu_{12} = 0.24, \rho = 2015\text{kg/m}^3 \tag{24}$$

Material II ([8], [9], [14], [15]):

$$E_1/E_2 = \text{open}, G_{12} = G_{13} = 0.6E_2, G_{23} = 0.5E_2, \nu_{12} = 0.25 \tag{25}$$

Material III ([14], [15]):

$$E_1/E_2 = \text{open}, G_{12} = G_{13} = 0.5E_2, G_{23} = 0.2E_2, \nu_{12} = 0.25 \tag{26}$$

Material IV [23]:

$$E_1 = 144.9\text{GPa}, E_2 = 9.65\text{GPa}, G_{12} = G_{13} = 4.14\text{GPa}, G_{23} = 3.45\text{GPa}, \nu_{12} = 0.3, \rho = 1389\text{kg/m}^3 \tag{27}$$

For convenience, the following non-dimensional terms are used in presenting the numerical results:

$$\overline{P}_{cr} = \begin{cases} \dfrac{P_{cr}L^2}{E_2bh^3} & \text{for Material II and III} \\ \dfrac{P_{cr}L^2}{E_1bh^3} & \text{for Material IV} \end{cases} \tag{28a}$$

$$\overline{\omega} = \begin{cases} \dfrac{\omega L^2}{h}\sqrt{\dfrac{\rho}{E_2}} & \text{for Material II and III} \\ \dfrac{\omega L^2}{h}\sqrt{\dfrac{\rho}{E_1}} & \text{for Material IV} \end{cases} \tag{28b}$$

As the first example, simply-supported symmetric cross-ply [90°/0°/0°/90°] composite beams with two span-to-height ratios ($L/h = 2.273$ and 22.73) are considered. The material properties are assumed to be Material I. The first five natural frequencies are tabulated in Table 1 along with numerical results of previous studies ([3], [7], [18]). The ABAQUS solutions given in Ref. [3] were obtained by using the plane stress element type CPS8 (quadrilateral element of eight node, 16 DOF per element). The differences between the natural frequencies calculated by the present formulation and those using different higher-order beam theories are very small.

In the next example, vibration and buckling analysis of simply-supported composite beams with with symmetric cross-ply [0°/90°/0°] and anti-symmetric cross-ply [0°/90°] lay-ups is performed. Material II and III with $E_1/E_2 = 10$ and 40 are used. The fundamental natural frequencies and critical buckling loads for different span-to-height ratios are compared with exact solutions ([8], [9]) and the finite elements results ([5], [14], [15]) in Tables 2 and 3. In the case of the FOBT, a value of 5/6 is used for the shear correction factor. An excellent agreement between the predictions of the present model and the results of the other models mentioned (FOBT and HOBT) can be observed. Material II with $E_1/E_2 = 40$ is chosen to show the effect of the axial force on the fundamental natural frequencies of beam with various L/h ratios (Fig. 2). It can be seen that the change of the natural frequency due to the axial force is noticeable. The natural frequency diminishes when the axial force changes from tensile to compressive, as expected. It is obvious that the natural frequency decreases with the increase of axial force, and the decrease becomes more quickly when the axial force is close to critical buckling load. For an anti-symmetric cross-ply lay-up, with $L/h = 5$, 10 and 20, at about P = 3.903, 4.936 and 5.290, respectively, the natural frequencies become zero which implies that at these loads, bucklings occur as a degenerate case of natural vibration at zero frequency. It also means that the buckling loads of composite beams under the axial force can be also obtained indirectly through vibration problem by increasing the axial force until the corresponding natural frequency vanishes. In order to show the effect of material anisotropy (E_1/E_2) on the critical buckling loads and the first four natural frequencies of a symmetric and an anti-symmetric cross-ply lay-up, a simply-supported composite beam with $L/h = 5$ is performed. It is observed that the critical buckling loads and natural frequencies increase with increasing orthotropy (Figs. 3 and 4). For a symmetric cross-ply lay-up, as ratio of E_1/E_2 increases, the order of the second and third vibration mode as well as the third and fourth vibration mode changes each other at $E_1/E_2 = 7$ and 27, respectively (Fig. 4).

To demonstrate the accuracy and validity of this study further, the fundamental natural frequencies of symmetric angle-ply $[\theta/-\theta]_s$ composite beams are given in Table 4 to illustrate the effect of boundary conditions and of fiber orientation. In the following examples, Material IV with $L/h = 15$ is used.

Variation of the critical buckling loads with respect to the fiber angle change is plotted in Fig. 5. The natural frequencies and buckling loads decrease monotonically with the increase of the fiber angle for all the boundary conditions considered. As the fiber angle increases, the buckling loads decrease more quickly than natural frequencies. For instant, the ratio between the buckling load at the fiber angle 0° and 90° is 9.8 and similar value for natural frequency is 3.0 for clamped-clamped boundary condition. It is observed that the present results are in good agreement with previous studies ([16], [23], [24], [25]) for all fiber angles.

In order to investigate the effects of fiber orientation on the natural frequencies, critical buckling loads and corresponding mode shapes, a simply-supported anti-symmetric angle-ply $[\theta/-\theta]$ composite beam is considered. The first four natural frequencies and critical buckling loads with respect to the fiber angle change are shown in Table 5 and Fig. 6. The uncoupled solution, which neglects the coupling effects coming from the material anisotropy, is also given. Due to coupling effects, the uncoupled solution might not be accurate. However, as the fiber angle increases, these effects become negligible. Therefore, it can be seen in Table 5 and Fig. 6 that the results by uncoupled and coupled solution are identical. For all fiber angles, the first four natural frequencies by the coupled solution exactly correspond to the first, second, third and fourth flexural mode by the uncoupled solution, respectively. It can be explained partly by the typical vibration mode shapes with the fiber angle $\theta = 45^\circ$ in Fig. 7. All the vibration modes exhibit double coupling (bending and shear components). It is indicated that the uncoupled solution is sufficiently accurate for an anti-symmetric angle-ply lay-up.

To investigate the coupling effects further, a clamped-clamped unsymmetric $[0^\circ/\theta]$ composite beam is chosen. As the fiber angle increases, major effects of coupling on the natural frequencies and critical buckling loads are seen in Table 6 and Fig. 8. The uncoupled and coupled solution shows discrepancy indicating the coupling effects become significant, especially at the higher fiber angles. The typical vibration mode shapes corresponding to the first four natural frequencies with the fiber angle $\theta = 60^\circ$ are illustrated in Fig. 9. The buckling mode shapes with various fiber angles $\theta = 30^\circ, 60^\circ$ and 90° are also given in Fig. 10. Relative measures of the axial and flexural displacements show that all the vibration and buckling modes are triply coupled mode (axial, bending and shear components). This fact explains as the fiber angle changes, the uncoupled solution disagrees with coupled solution as anisotropy of the beam gets higher. That is, the uncoupled solution is no longer valid for unsymmetrically laminated composite beams, and triply extension-bending-shear coupled vibration and buckling should be considered simultaneously for accurate analysis of composite beams.

8. Conclusions

A two-noded C^1 beam element of five degree-of-freedom per node is developed to study the vibration and buckling behaviour of composite beams using refined shear deformation theory. This model is capable of predicting accurately the natural frequencies, critical buckling loads and corresponding mode shapes. It accounts for the parabolical variation of shear strains through the depth of the beam, and satisfies the zero traction boundary conditions on the top and bottom surfaces of the beam without using shear correction factor. The uncoupled solution is accurate for lower degrees of material anisotropy, but, becomes inappropriate as the anisotropy of the beam gets higher, and triply extension-bending-shear coupled vibration and buckling should be considered simultaneously for accurate analysis of composite beams. The present model is found to be appropriate and efficient in analyzing vibration and buckling problem of composite beams.

9. References

References

[1] K. Chandrashekhara, K. Bangera, Free vibration of composite beams using a refined shear flexible beam element, Computers and Structures 43 (4) (1992) 719 – 727.

[2] S. R. Marur, T. Kant, Free vibration analysis of fiber reinforced composite beams using higher order theories and finite element modelling, Journal of Sound and Vibration 194 (3) (1996) 337 – 351.

[3] M. Karama, B. A. Harb, S. Mistou, S. Caperaa, Bending, buckling and free vibration of laminated composite with a transverse shear stress continuity model, Composites Part B: Engineering 29 (3) (1998) 223 – 234.

[4] G. Shi, K. Y. Lam, Finite element vibration analysis of composite beams based on higher-order beam theory, Journal of Sound and Vibration 219 (4) (1999) 707 – 721.

[5] M. V. V. S. Murthy, D. R. Mahapatra, K. Badarinarayana, S. Gopalakrishnan, A refined higher order finite element for asymmetric composite beams, Composite Structures 67 (1) (2005) 27 – 35.

[6] P. Subramanian, Dynamic analysis of laminated composite beams using higher order theories and finite elements, Composite Structures 73 (3) (2006) 342 – 353.

[7] P. Vidal, O. Polit, A family of sinus finite elements for the analysis of rectangular laminated beams, Composite Structures 84 (1) (2008) 56 – 72.

[8] A. A. Khdeir, J. N. Reddy, Free vibration of cross-ply laminated beams with arbitrary boundary conditions, International Journal of Engineering Science 32 (12) (1994) 1971–1980, cited By (since 1996) 47.

[9] A. A. Khdeir, J. N. Reddy, Buckling of cross-ply laminated beams with arbitrary boundary conditions, Composite Structures 37 (1) (1997) 1 – 3.

[10] T. Kant, S. R. Marur, G. Rao, Analytical solution to the dynamic analysis of laminated beams using higher order refined theory, Composite Structures 40 (1) (1997) 1 – 9.

[11] T. Kant, K. Swaminathan, Analytical solutions for free vibration of laminated composite and sandwich plates based on a higher-order refined theory, Composite Structures 53 (1) (2001) 73 – 85.

[12] W. Zhen, C. Wanji, An assessment of several displacement-based theories for the vibration and stability analysis of laminated composite and sandwich beams, Composite Structures 84 (4) (2008) 337 – 349.

[13] H. Matsunaga, Vibration and buckling of multilayered composite beams according to higher order deformation theories, Journal of Sound and Vibration 246 (1) (2001) 47 – 62.

[14] M. Aydogdu, Vibration analysis of cross-ply laminated beams with general boundary conditions by Ritz method, International Journal of Mechanical Sciences 47 (11) (2005) 1740 – 1755.

[15] M. Aydogdu, Buckling analysis of cross-ply laminated beams with general boundary conditions by Ritz method, Composites Science and Technology 66 (10) (2006) 1248 – 1255.

[16] M. Aydogdu, Free vibration analysis of angle-ply laminated beams with general boundary conditions, Journal of Reinforced Plastics and Composites 25 (15) (2006) 1571–1583.

[17] L. Jun, L. Xiaobin, H. Hongxing, Free vibration analysis of third-order shear deformable composite beams using dynamic stiffness method, Archive of Applied Mechanics 79 (2009) 1083–1098.

[18] L. Jun, H. Hongxing, Free vibration analyses of axially loaded laminated composite beams based on higher-order shear deformation theory, Meccanica 46 (2011) 1299–1317.

[19] T. P. Vo and H. T. Thai, Static behaviour of composite beams using various refined shear deformation theories. Composite Structures 94 (8) (2012) 2513–2522

[20] R. P. Shimpi, Refined plate theory and its variants, AIAA Journal 40 (1) (2002) 137–146

[21] R. P. Shimpi, H. G. Patel, A two variable refined plate theory for orthotropic plate analysis, International Journal of Solids and Structures 43 (22-23) (2006) 6783–6799

[22] R. M. Jones, Mechanics of Composite Materials, Taylor & Francis, 1999.

[23] K. Chandrashekhara, K. Krishnamurthy, S. Roy, Free vibration of composite beams including rotary inertia and shear deformation, Composite Structures 14 (4) (1990) 269 – 279.

[24] S. Krishnaswamy, K. Chandrashekhara, W. Z. B. Wu, Analytical solutions to vibration of generally layered composite beams, Journal of Sound and Vibration 159 (1) (1992) 85 – 99.

[25] W. Q. Chen, C. F. Lv, Z. G. Bian, Free vibration analysis of generally laminated beams via state-space-based differential quadrature, Composite Structures 63 (3-4) (2004) 417 – 425.

Figure 1: Geometry of a laminated composite beam.

Figure 2: The interaction diagram between non-dimensional critical buckling load and fundamental natural frequency of a simply supported symmetric and anti-symmetric cross-ply composite beam with $L/h = 5$, 10 and 20.

Figure 3: Effect of material anisotropy on the non-dimensional critical buckling loads of a simply supported symmetric and anti-symmetric cross-ply composite beam with $L/h = 5$.

Figure 4: Effect of material anisotropy on the first five non-dimensional natural frequencies of a simply supported symmetric and anti-symmetric cross-ply composite beam with $L/h = 5$.

Figure 5: Variation of the non-dimensional critical buckling loads of symmetric angle-ply $[\theta/-\theta]_s$ composite beams with respect to the fiber angle change.

Figure 6: Variation of the non-dimensional critical buckling loads of a simply-supported anti-symmetric angle-ply $[\theta/-\theta]$ composite beam with respect to the fiber angle change.

Figure 7: Vibration mode shapes of the axial and flexural components of a simply-supported composite beam with the fiber angle 45°.

Figure 8: Variation of the non-dimensional critical buckling loads of a clamped-clamped unsymmetric $[0^\circ/\theta]$ composite beam with respect to the fiber angle change.

Figure 9: Vibration mode shapes with the axial and flexural components of a clamped-clamped composite beam with the fiber angle 60°.

Figure 10: Bucking mode shapes with the axial and flexural components of a clamped-clamped composite beam with the fiber angles 30°, 60° and 90°.

Table 1: The first five fundamental natural frequencies (Hz) of simply-supported beams with a symmetric cross-ply $[90^\circ/0^\circ/0^\circ/90^\circ]$ lay-up (L/h=2.273 and 22.73, Material I).

Table 2: Effect of span-to-height ratios on the non-dimensional fundamental natural frequencies of a symmetric and an anti-symmetric cross-ply composite beam with simply-supported boundary condition (Material II with $E_1/E_2 = 40$).

Table 3: Effect of span-to-height ratios on the non-dimensional critical buckling loads of a symmetric and an anti-symmetric cross-ply composite beam with simply-supported boundary condition (Material II and III with $E_1/E_2 = 10$ and 40).

Table 4: The non-dimensional fundamental frequencies of symmetric angle-ply $[\theta/-\theta]_s$ composite beams with respect to the fiber angle change ($L/h = 15$, Material IV).

Table 5: The first four non-dimensional frequencies of anti-symmetric angle-ply $[\theta/-\theta]$ composite beams with respect to the fiber angle change ($L/h = 15$, Material IV).

Table 6: The first four non-dimensional frequencies of unsymmetric $[0^\circ/\theta]$ composite beams with respect to the fiber angle change ($L/h = 15$, Material IV).

CAPTIONS OF TABLES

Table 1: The first five natural frequencies (Hz) of simply-supported beams with a symmetric cross-ply $[90^0 / 0^0 / 0^0 / 90^0]$ lay-up (Material I with L/h=2.273 and 22.73).

Table 2: Effect of span-to-height ratios on the non-dimensional fundamental natural frequencies of a symmetric and an anti-symmetric cross-ply composite beam with simply-supported boundary condition (Material II with $E_1/E_2 = 40$).

Table 3: Effect of span-to-height ratios on the non-dimensional critical buckling loads of a symmetric and an anti-symmetric cross-ply composite beam with simply-supported boundary condition (Material II and III with $E_1/E_2 = 10$).

Table 4: Effect of span-to-height ratios on the non-dimensional critical buckling loads of a symmetric and an anti-symmetric cross-ply composite beam with simply-supported boundary condition (Material II and III with $E_1/E_2 = 40$).

Table 5: The non-dimensional fundamental natural frequencies of symmetric angle-ply $[\theta / -\theta]_s$ composite beams with respect to the fiber angle change (Material IV with L/h = 15).

Table 6: The first four non-dimensional natural frequencies of a simply-supported anti-symmetric angle-ply $[\theta / -\theta]$ composite beam with respect to the fiber angle change (Material IV with L/h = 15).

Table 7: The first four non-dimensional natural frequencies of an unsymmetric $[0 / \theta]$ clamped-clamped composite beam with respect to the fiber angle change (Material IV with L/h = 15).

Table 1: The first five natural frequencies (Hz) of simply-supported beams with a symmetric cross-ply $[90^0 / 0^0 / 0^0 / 90^0]$ lay-up (Material I with L/h=2.273 and 22.73).

Mode	L/h = 2.273				L/h = 22.73				
	ABAQUS [3]	Ref. [3]	Ref. [7]	Present	ABAQUS [3]	Ref. [3]	Ref. [7]	Ref. [18]	Present
1	82.90	83.70	82.81	82.42	14.95	14.96	14.97	14.97	14.42
2	200.60	195.80	195.62	195.20	57.60	57.90	57.85	57.87	55.88
3	324.30	313.40	319.36	315.88	122.80	123.70	123.55	123.58	119.76
4	450.10	441.80	460.18	449.83	204.20	206.40	206.18	206.01	200.44
5	576.40	583.80	515.41	578.65	296.60	300.60	300.71	299.68	292.73

Table 2: Effect of span-to-height ratios on the non-dimensional fundamental natural frequencies of a symmetric and an anti-symmetric cross-ply composite beam with simply-supported boundary condition (Material II with $E_1/E_2 = 40$).

Lay-ups	Theory	Reference	L/h			
			5	10	20	50
$[0^0/90^0/0^0]$	FOBT	Khdeir and Reddy [8]	9.205	13.670	-	-
		Present	9.205	13.665	16.359	17.456
	HOBT	Murthy et al. [5]	9.207	13.614	-	-
		Khdeir and Reddy [8]	9.208	13.614	-	-
		Aydogdu [14]	9.207	-	16.337	-
		Present	9.206	13.607	16.327	17.449
$[0^0/90^0]$	FOBT	Khdeir and Reddy [8]	5.953	6.886	-	-
		Present	5.886	6.848	7.187	7.294
	HOBT	Murthy et al. [5]	6.045	6.908	-	-
		Khdeir and Reddy [8]	6.128	6.945	-	-
		Aydogdu [14]	6.144	-	7.218	-
		Present	6.058	6.909	7.204	7.296

Table 3: Effect of span-to-height ratios on the non-dimensional critical buckling loads of a symmetric and an anti-symmetric cross-ply composite beam with simply-supported boundary condition (Material II and III with $E_1/E_2 = 10$).

Lay-ups	Theory	Reference	L/h			
			5	10	20	50
Material II						
$[0^0/90^0/0^0]$	FOBT	Present	4.752	6.805	7.630	7.897
	HOBT	Aydogdu [15]	4.726	-	7.666	-
		Present	4.709	6.778	7.620	7.896
$[0^0/90^0]$	FOBT	Present	1.883	2.148	2.226	2.249
	HOBT	Aydogdu [15]	1.919	-	2.241	-
		Present	1.910	2.156	2.228	2.249
Material III						
$[0^0/90^0/0^0]$	FOBT	Present	4.069	6.420	7.503	7.875
	HOBT	Aydogdu [15]	3.728	-	7.459	-
		Present	3.717	6.176	7.416	7.860
$[0^0/90^0]$	FOBT	Present	1.605	1.876	1.958	1.983
	HOBT	Aydogdu [15]	1.765	-	2.226	-
		Present	1.758	2.104	2.214	2.247

Table 4: Effect of span-to-height ratios on the non-dimensional critical buckling loads of a symmetric and an anti-symmetric cross-ply composite beam with simply-supported boundary condition (Material II and III with $E_1/E_2 = 40$).

Lay-ups	Theory	Reference	L/h			
			5	10	20	50
Material II						
$[0^0/90^0/0^0]$	FOBT	Khdeir and Reddy [9]	8.606	18.989	-	-
		Present	8.604	18.974	27.154	30.882
	HOBT	Khdeir and Reddy [9]	8.613	18.832	-	-
		Aydogdu [15]	8.613	-	27.084	-
		Present	8.609	18.814	27.050	30.859
$[0^0/90^0]$	FOBT	Present	3.680	4.848	5.265	5.395
	HOBT	Aydogdu [15]	3.906	-	5.296	-
		Present	3.903	4.936	5.290	5.399
Material III						
$[0^0/90^0/0^0]$	FOBT	Present	6.600	16.253	25.620	30.549
	HOBT	Aydogdu [15]	5.896	-	24.685	-
		Present	5.895	14.857	24.655	30.319
$[0^0/90^0]$	FOBT	Present	3.110	4.571	5.180	5.381
	HOBT	Aydogdu [15]	3.376	-	5.225	-
		Present	3.373	4.697	5.219	5.387

Table 5: The non-dimensional fundamental natural frequencies of symmetric angle-ply $[\theta/-\theta]_s$ composite beams with respect to the fiber angle change (Material IV with L/h = 15).

Boundary conditions	Reference	Fiber angle θ						
		0^0	15^0	30^0	45^0	60^0	75^0	90^0
CC	Aydogdu [16]	4.9730	4.2940	2.1950	1.9290	1.6690	1.6120	1.6190
	Chandrashekhara et al. [23]	4.8487	4.6635	4.0981	3.1843	2.1984	1.6815	1.6200
	Krishnaswamy et al. [24]	4.8690	3.9880	2.8780	1.9470	1.6690	1.6120	1.6190
	Chen et al. [25]	4.8575	3.6484	2.3445	1.8383	1.6711	1.6161	1.6237
	Present	4.8969	4.5695	3.2355	1.9918	1.6309	1.6056	1.6152
SS	Aydogdu [16]	2.6510	1.8960	1.1410	0.8040	0.7360	0.7250	0.7290
	Chandrashekhara et al. [23]	2.6560	2.5105	2.1032	1.5368	1.0124	0.7611	0.7320
	Present	2.6494	2.4039	1.5540	0.9078	0.7361	0.7247	0.7295
CF	Aydogdu [16]	0.9810	0.6760	0.4140	0.2880	0.2620	0.2580	0.2600
	Chandrashekhara et al. [23]	0.9820	0.9249	0.7678	0.5551	0.3631	0.2723	0.2619
	Present	0.9801	0.8836	0.5614	0.3253	0.2634	0.2593	0.2611
CS	Aydogdu [16]	3.7750	2.9600	1.6710	1.1780	1.1500	1.1220	1.1290
	Chandrashekhara et al. [23]	3.7310	3.5590	3.0570	2.3030	1.5510	1.1750	1.1360
	Krishnaswamy et al. [24]	3.8370	3.2430	2.2130	1.3880	1.1460	1.1290	1.1310
	Present	3.8183	3.5079	2.3538	1.4019	1.1407	1.1231	1.1302

Table 6: The first four non-dimensional natural frequencies of a simply-supported anti-symmetric angle-ply $[\theta/-\theta]$ composite beam with respect to the fiber angle change (Material IV with L/h = 15).

Fiber angle	No coupling				With coupling			
	ω_{z_1}	ω_{z_2}	ω_{z_3}	ω_{z_4}	ω_1	ω_2	ω_3	ω_4
0^0	2.6494	8.9572	16.6431	24.7032	2.6494	8.9572	16.6431	24.7032
15^0	2.4039	8.3223	15.7685	23.7045	2.4039	8.3223	15.7685	23.7045
30^0	1.5540	5.7944	11.8313	18.8714	1.5540	5.7944	11.8313	18.8714
45^0	0.9078	3.5255	7.5850	12.7587	0.9078	3.5255	7.5850	12.7587
60^0	0.7361	2.8798	6.2616	10.6606	0.7361	2.8798	6.2616	10.6606
75^0	0.7247	2.8352	6.1639	10.4930	0.7247	2.8352	6.1639	10.4930
90^0	0.7295	2.8526	6.1977	10.5426	0.7295	2.8526	6.1977	10.5426

Table 7: The first four non-dimensional natural frequencies of an unsymmetric $[0/\theta]$ clamped-clamped composite beam with respect to the fiber angle change (Material IV with L/h = 15).

Fiber angle	No coupling				With coupling			
	ω_{z_1}	ω_{z_2}	ω_{z_3}	ω_{z_4}	ω_1	ω_2	ω_3	ω_4
0^0	4.897	11.493	18.400	26.448	4.897	11.493	18.400	26.448
15^0	4.742	11.212	18.037	26.011	4.730	11.192	18.015	25.988
30^0	4.272	10.330	16.901	24.637	3.957	9.744	16.218	23.893
45^0	4.009	9.802	16.192	23.743	3.108	7.967	13.886	21.042
60^0	3.950	9.665	15.977	23.437	2.859	7.400	13.071	19.975
75^0	3.938	9.625	15.896	23.306	2.840	7.351	12.984	19.841
90^0	3.935	9.615	15.872	23.264	2.846	7.361	12.992	19.844

CAPTIONS OF FIGURES

Figure 1: Geometry of a laminated composite beam.

Figure 2: The interaction diagram between non-dimensional critical buckling load and fundamental natural frequency of a symmetric and an anti-symmetric cross-ply composite beam with simply-supported boundary condition (Material II with L/h = 5, 10 and 20).

Figure 3: Effect of material anisotropy on the non-dimensional critical buckling loads of a symmetric and an anti-symmetric cross-ply composite beam with simply-supported boundary condition (Material II with L/h = 5).

Figure 4: Effect of material anisotropy on the first four non-dimensional natural frequencies of a symmetric and an anti-symmetric cross-ply composite beam with simply-supported boundary condition (Material II with L/h = 5).

Figure 5: Variation of the non-dimensional critical buckling loads of symmetric angle-ply $[\theta/-\theta]_s$ composite beams with respect to the fiber angle change (Material IV with L/h = 15).

Figure 6: Variation of the non-dimensional critical buckling loads of a simply-supported anti-symmetric angle-ply $[\theta/-\theta]$ composite beam with respect to the fiber angle change (Material IV with L/h = 15).

Figure 7: Vibration mode shapes with the axial and flexural components of a simply-supported composite beam with the fiber angle 45^0

Figure 8: Variation of the non-dimensional critical buckling loads of a clamped-clamped unsymmetric $[0/\theta]$ composite beam with respect to the fiber angle change (Material IV with L/h = 15).

Figure 9: Vibration mode shapes with the axial and flexural components of a clamped-clamped composite beam with the fiber angle 60^0.

Figure 10: Bucking mode shapes with the axial and flexural components of a clamped-clamped composite beam with the fiber angles 30^0, 60^0 and 90^0.

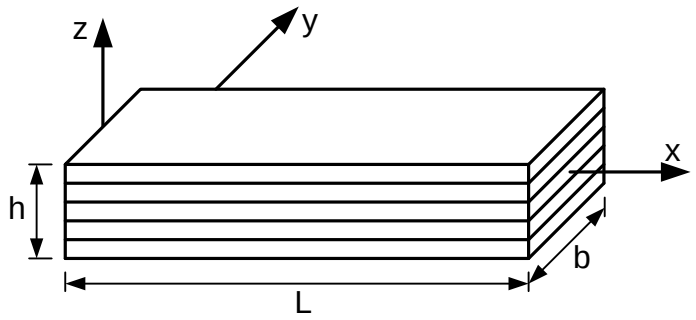

Figure 1: Geometry of a laminated composite beam.

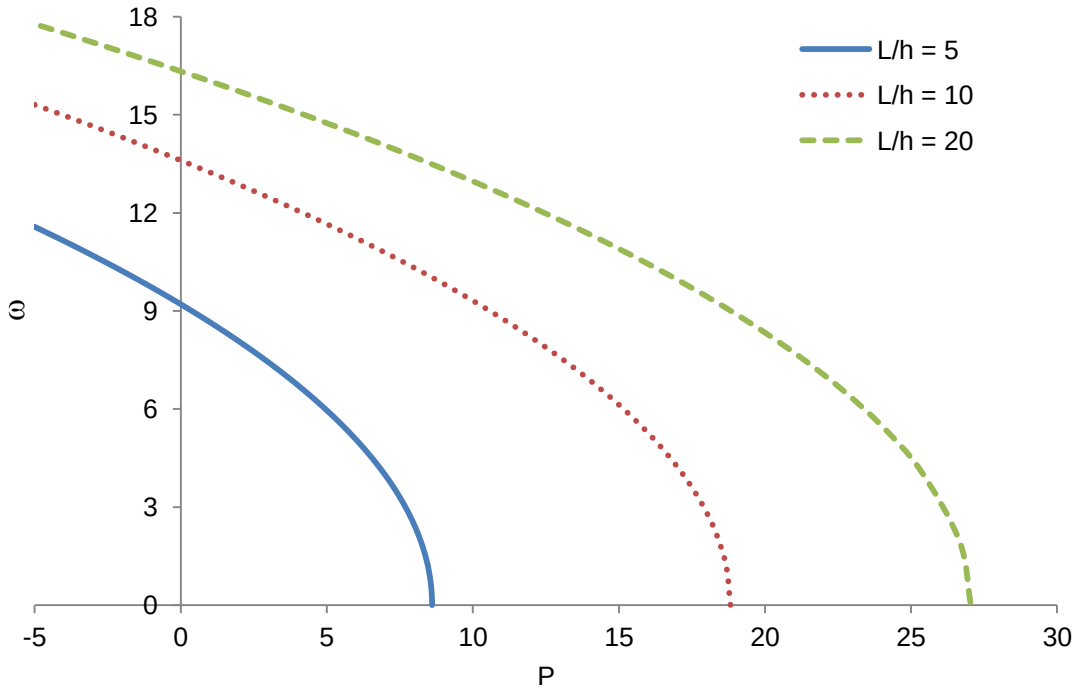

a. Symmetric cross-ply lay-up ($[0^0/90^0/0^0]$)

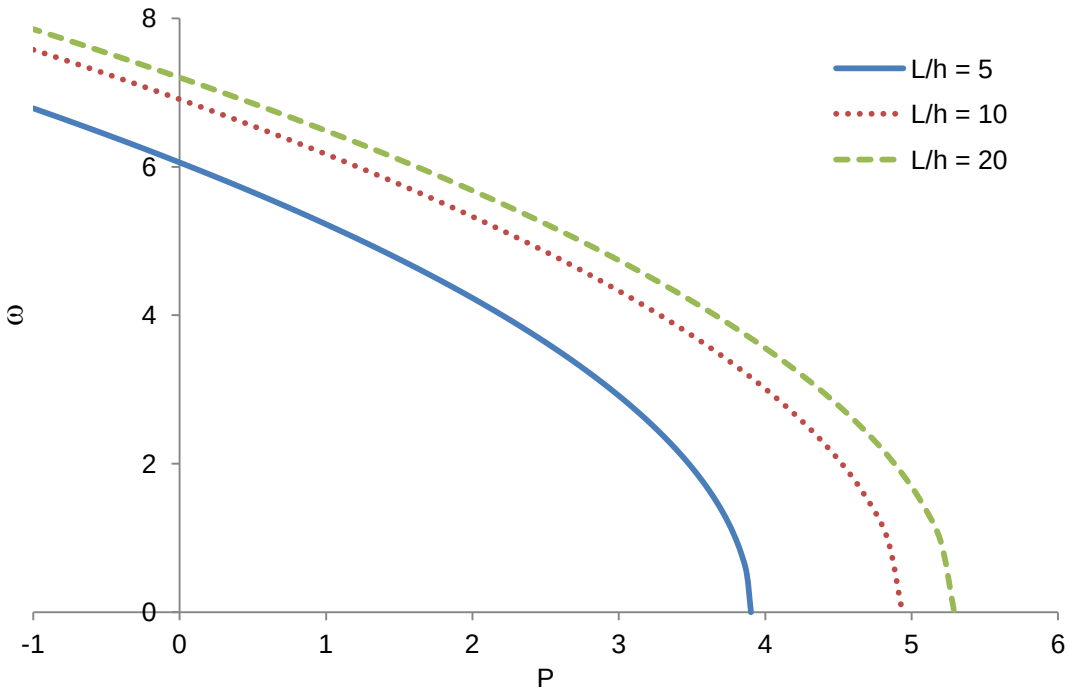

b. Anti-symmetric cross-ply lay-up ($[0^0/90^0]$)

Figure 2: The interaction diagram between non-dimensional critical buckling load and fundamental natural frequency of a symmetric and an anti-symmetric cross-ply composite beam with simply-supported boundary condition (Material II with L/h = 5, 10 and 20).

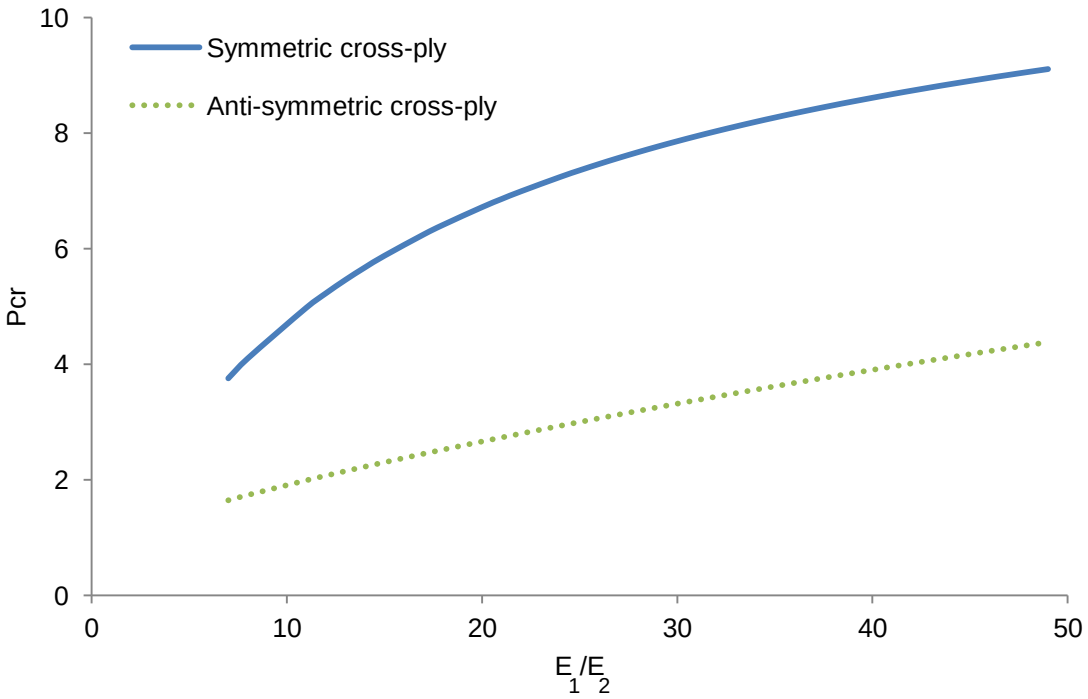

Figure 3: Effect of material anisotropy on the non-dimensional critical buckling loads of a symmetric and an anti-symmetric cross-ply composite beam with simply-supported boundary condition (Material II with L/h = 5).

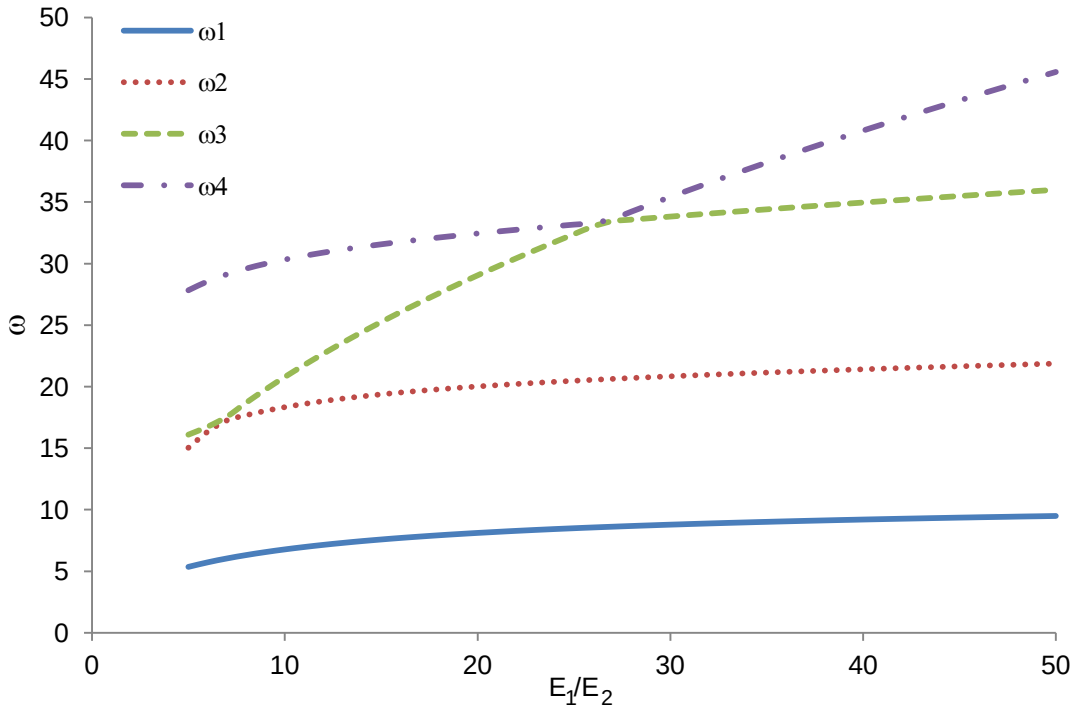

a. Symmetric cross-ply lay-up ($[0^0/90^0/0^0]$)

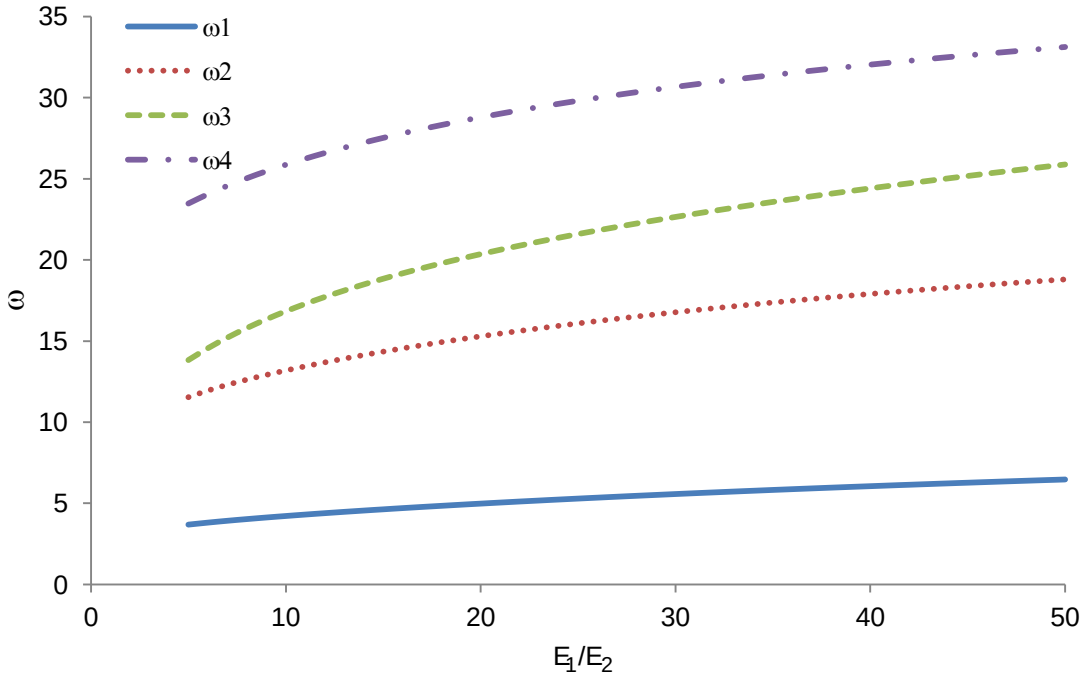

b. Anti-symmetric cross-ply lay-up ($[0^0/90^0]$)

Figure 4: Effect of material anisotropy on the first four non-dimensional natural frequencies of a symmetric and an anti-symmetric cross-ply composite beam with simply-supported boundary condition (Material II with L/h = 5).

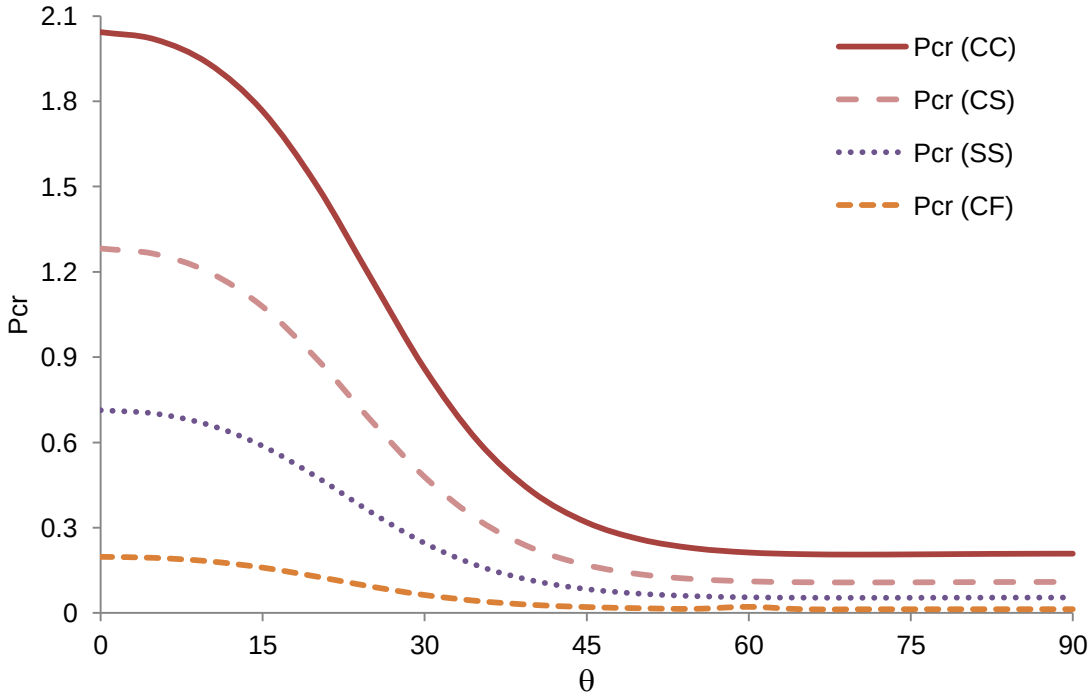

Figure 5: Variation of the non-dimensional critical buckling loads of symmetric angle-ply $[\theta/-\theta]_s$ composite beams with respect to the fiber angle change (Material IV with L/h = 15).

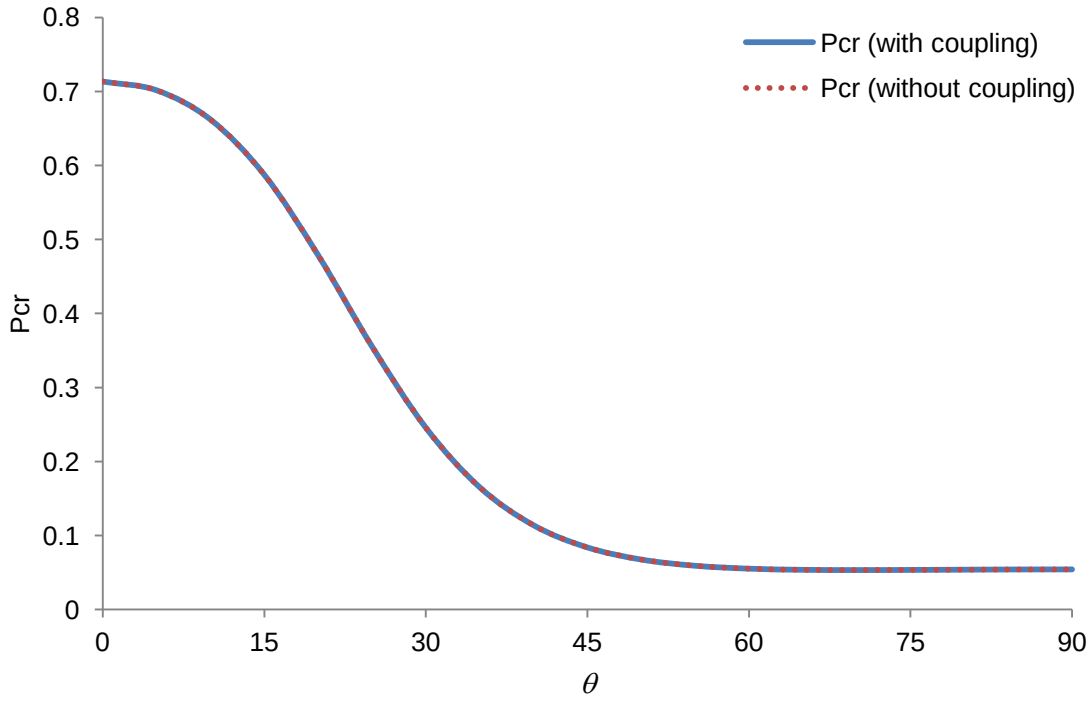

Figure 6: Variation of the non-dimensional critical buckling loads of a simply-supported anti-symmetric angle-ply $[\theta/-\theta]$ composite beam with respect to the fiber angle change (Material IV with L/h = 15).

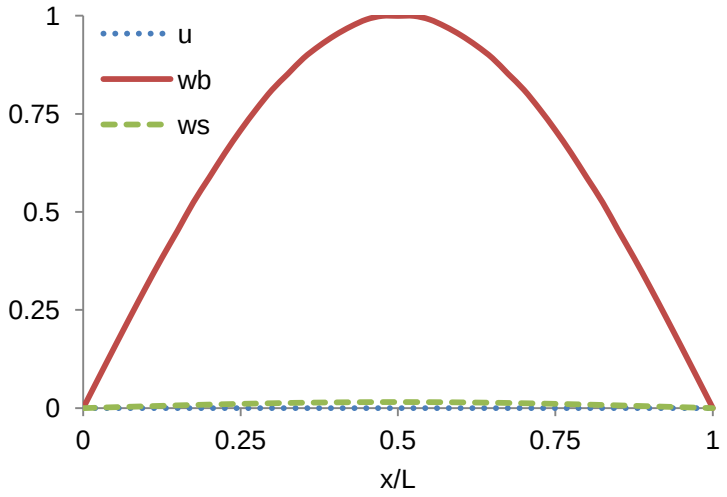

a. Fundamental mode shape $\omega_1 = 0.9078$.

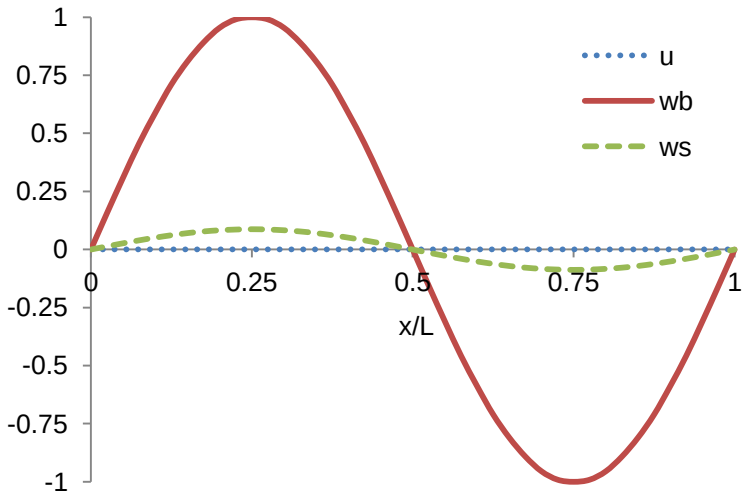

b. Second mode shape $\omega_2 = 3.5255$.

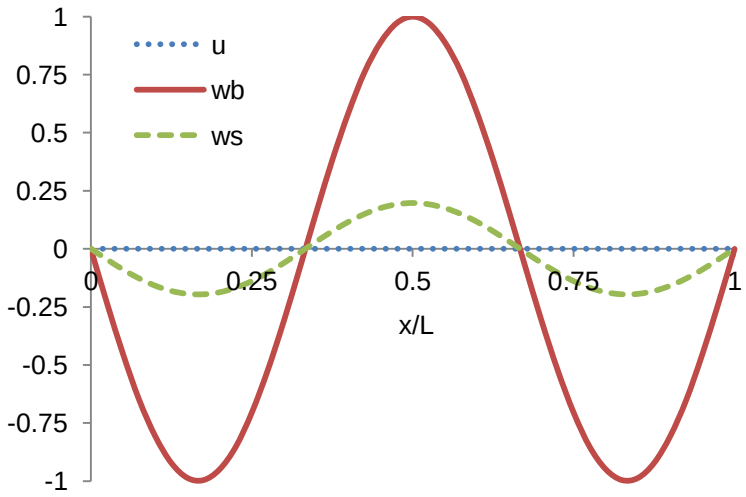

c. Third mode shape $\omega_3 = 7.5850$.

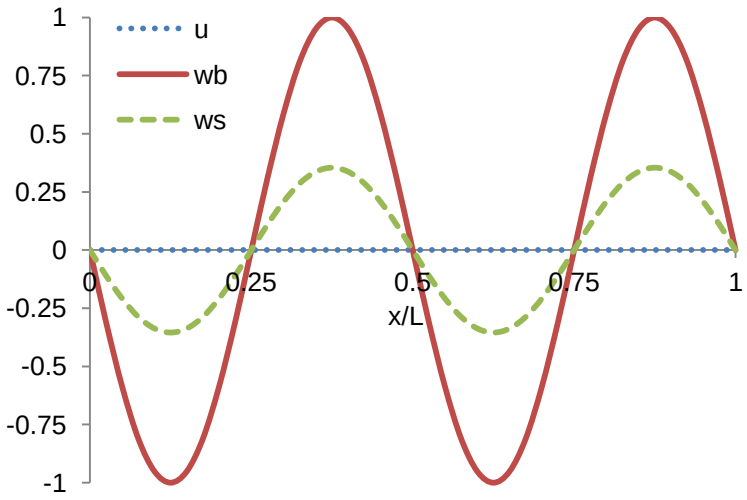

d. Fourth mode shape $\omega_4 = 12.7587$

Figure 7: Vibration mode shapes with the axial and flexural components of a simply-supported composite beam with the fiber angle 45^0

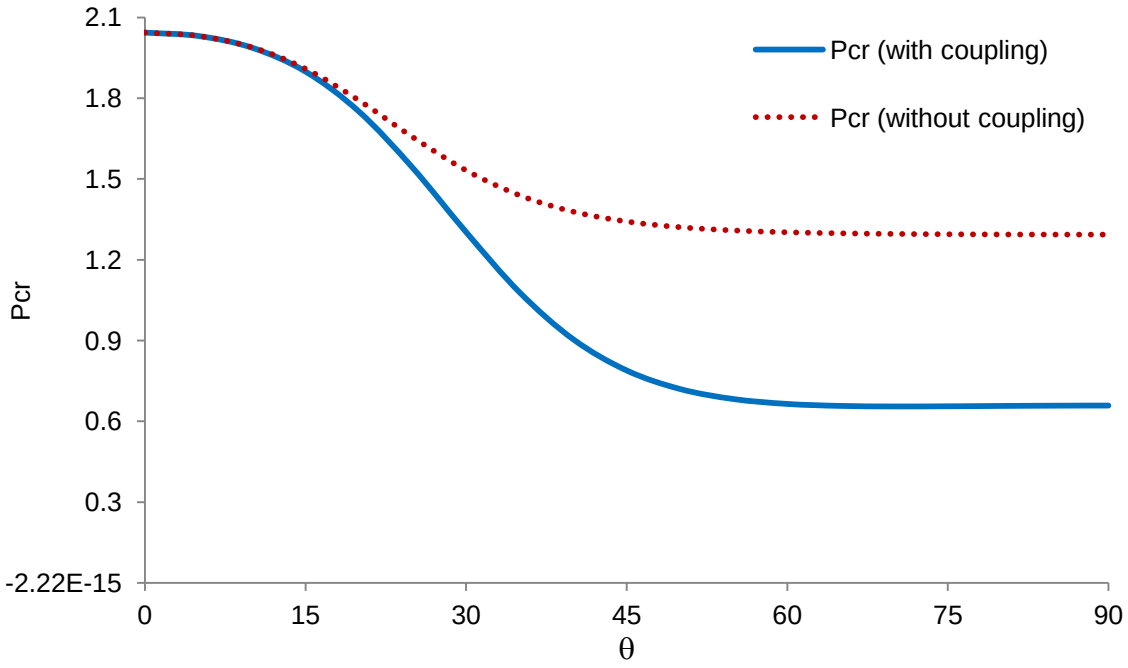

Figure 8: Variation of the non-dimensional critical buckling loads of a clamped-clamped unsymmetric $[0/\theta]$ composite beam with respect to the fiber angle change (Material IV with L/h = 15).

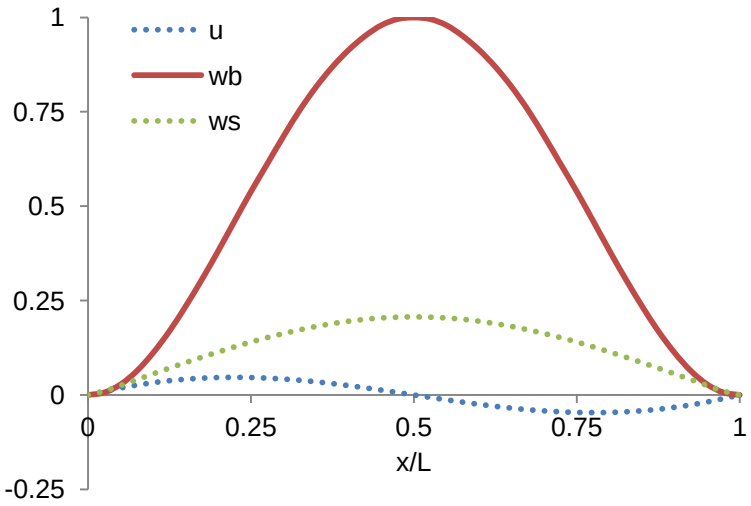

a. Fundamental mode shape $\omega_1 = 2.859$.

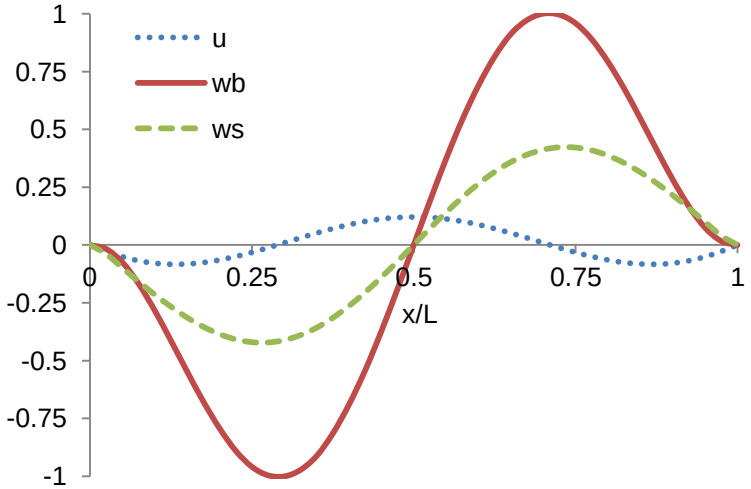

b. Second mode shape $\omega_2 = 7.400$.

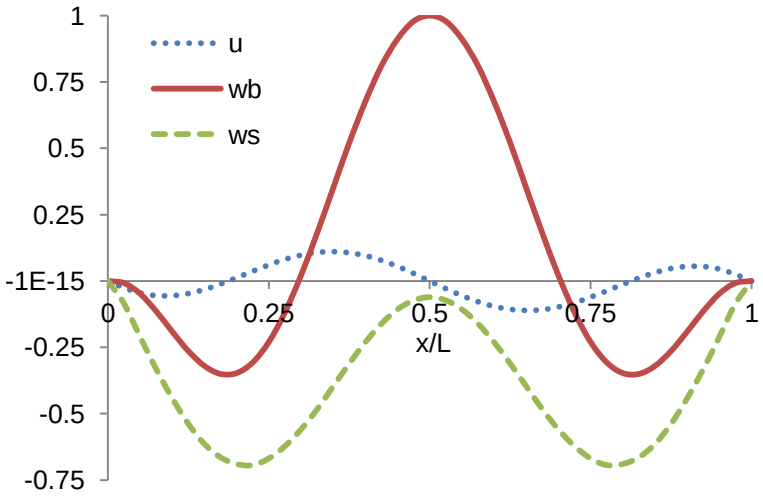

c. Third mode shape $\omega_3 = 13.071$.

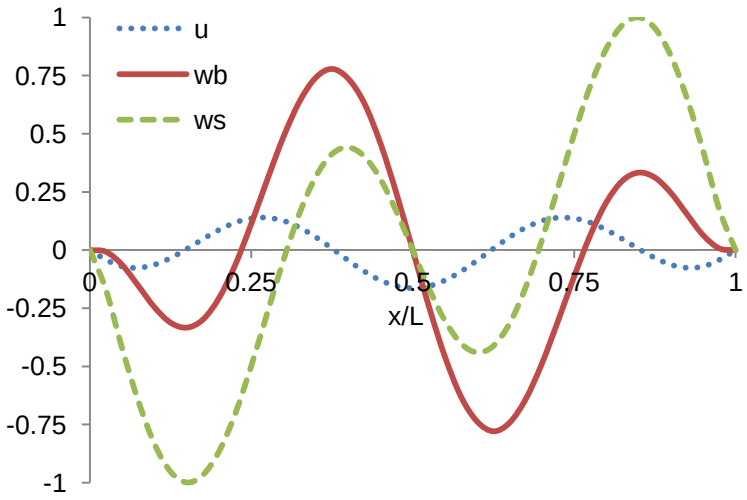

d. Fourth mode shape $\omega_4 = 19.975$

Figure 9: Vibration mode shapes with the axial and flexural components of a clamped-clamped composite beam with the fiber angle 60^0.

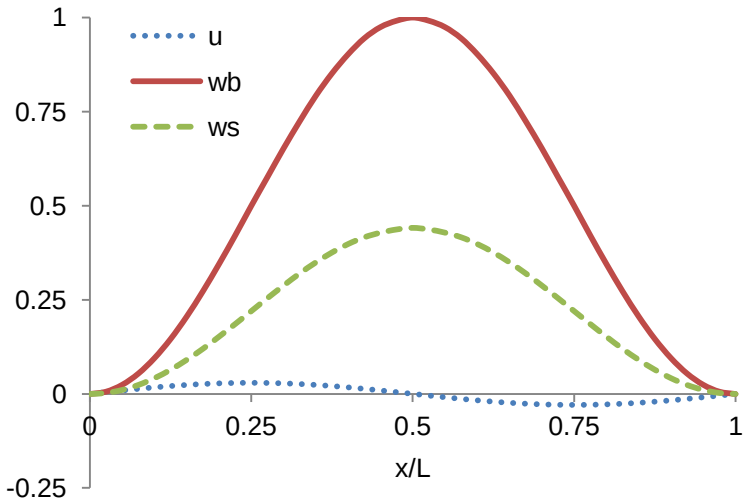

a. P_{cr} = 1.3028 with the fiber angle 30^0.

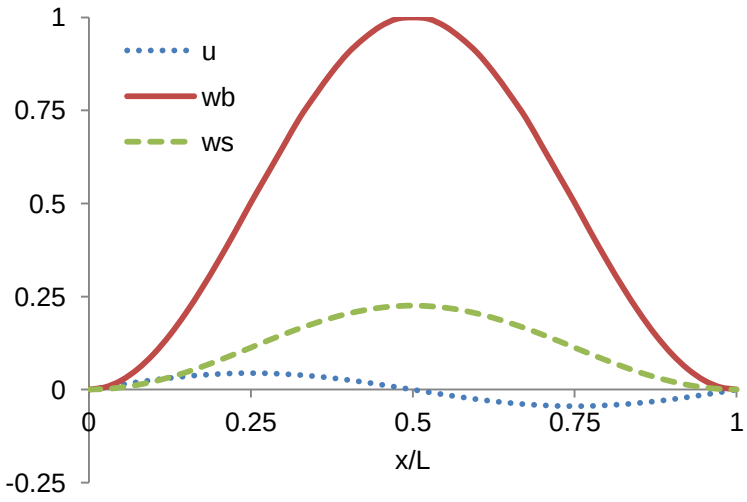

b. P_{cr} = 0.7888 with the fiber angle 45^0.

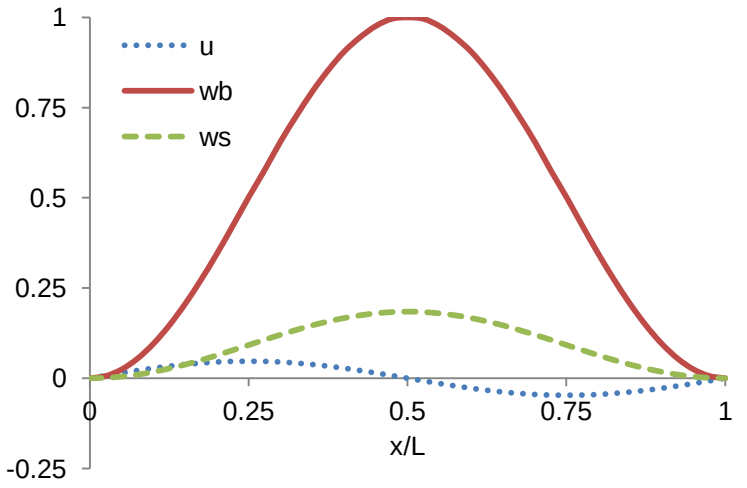

c. P_{cr} = 0.6585 with the fiber angle 90^0.

Figure 10: Bucking mode shapes with the axial and flexural components of a clamped-clamped composite beam with the fiber angles 30^0, 60^0 and 90^0.